Template Synthesis of Near-Monodisperse[1] Microscale Nanofibers and Nanotubules of MoS_2

Catherine M. Zelenski and Peter K. Dorhout*,[2]

Contribution from the Department of Chemistry, Colorado State University, Fort Collins, Colorado 80523

Received June 30, 1997

Abstract: Near-monodisperse microscopic nanostructures of MoS_2 were prepared by thermal decomposition of two different ammonium thiomolybdate molecular precursors, $(NH_4)_2MoS_4$ and $(NH_4)_2Mo_3S_{13}$, within the confined voids of a porous aluminum oxide membrane template. Our low-temperature (450 °C) synthetic route yielded large quantities of hollow tubules of MoS_2 of uniform size and shape that were ∼30 μm long with diameters of 50 nm and wall thicknesses of about 10 nm. More irregularly shaped, mainly solid fibers of MoS_2 with diameters of about 200 nm were synthesized by changing the template to one with larger pores. The morphology of the fibers or tubules was studied with respect to the choice of precursor, the characteristics of the precursor solutions, the incorporation methods, the template characteristics, and the heat treatment during firing. The MoS_2 structures were characterized by scanning and transmission electron microscopies, energy dispersive spectroscopy, electron and X-ray diffraction, and optical absorption spectroscopy. This template-assisted growth process yielded large quantities of MoS_2 tubules or fibers that could be isolated from the template. However, under the growth conditions studied, the formation of H_xMoS_2 "bronzes" could not be discounted.

Introduction

The family of layered metal chalcogenides, MQ_2, is known to adopt a number of packing structures resulting in either trigonal prismatic or octahedral coordination of the metals within a layered matrix of chalcogens.[3] Known forms for molybdenum sulfides include the 1T- and 2H-types. In their bulk form, the quasi-infinite metal sulfide sheets stack one above the other, held together through van der Waals interactions, to create tremendously stable phases, 2H−MoS_2, as an example. This compound, in particular, is known to be a useful catalyst for hydrodesulfurization,[4−7] an electrode in high energy density batteries,[8] and an intercalation host to form new materials.[9−13] For each of these applications, the important processes occur either at the surface or at the exposed edges of the MoS_2 layers. Nanoclusters of MoS_2 would provide a tremendously increased surface area of exposed edges on which to perform chemistry.

The concept of MS_2 nanoclusters and tubules (M = Mo, W) has been beautifully demonstrated by the group of Tenne.[14−22] Their processes involved the production of macroscopic quantities of fullerene-like nanotubules and negative-curvature polyhedra, or nested inorganic fullerene-like clusters, through the reduction of an appropriate metal oxide precursor by an H_2/H_2S mixture at temperatures above 800 °C. They have shown that, left to their own devices in the gas phase, nanoparticles and nanotubules of MS_2 form as "onion-skin clusters"[23] or "nested clusters and tubules" that are often spherical or cylindrical in appearance and are hollow in the center.[19] Although they have extensively studied the reaction mechanisms associated with particle formation from the gas phase and the intercalation of these particles with other metal atoms,[15,17] they have not been able to control the size or size distribution of the nanospheres or nanotubules, which often range from ∼7 to over several hundred nanometers in diameter within a single syn-

* To whom correspondence should be addressed.

(1) A definition of "near-monodisperse" nanoparticles can be found in: Aiken, J. D., III; Lin, Y.; Finke, R. G. *J. Mol. Catal. A: Chem.* **1996**, *114*, 29−51.

(2) Alfred P. Sloan Fellow, 1997−1999; Camille Dreyfus Teacher Scholar, 1997. E-mail: pkd@LAMAR.colostate.edu.

(3) Hulliger, F. *Structural Chemistry of Layer-Type Phases*; Reidel: Dordrecht, 1976; p 377.

(4) Müller, A. *Polyhedron* **1986**, *5*, 323−340.

(5) Miremadi, B. K.; Morrison, S. R. *J. Catal.* **1987**, *103*, 334−345.

(6) Dejong, A. M.; Debeer, V. H. J.; Vanveen, J. A. R.; Niemantsverdriet, J. W. *J. Phys. Chem.* **1996**, *100*, 17722−17724.

(7) Okamoto, Y.; Katsuyama, H.; Yoshida, K.; Nakai, K.; Matsuo, M.; Sakamoto, Y.; Yu, J. H.; Terasaki, O. *J. Chem. Soc., Faraday Trans.* **1996**, *92*, 4647−4656.

(8) Ruizhitzky, E.; Jimenez, R.; Casal, B.; Manriquez, V.; Ana, A. S.; Gonzalez, G. *Adv. Mater.* **1993**, *5*, 738−741.

(9) Gee, M. A.; Frindt, R. F.; Joensen, P.; Morrison, S. R. *Mater. Res. Bull.* **1986**, *21*, 543−549.

(10) Divigalpitiya, W. M. R.; Frindt, R. F.; Morrison, S. R. *Science* **1989**, *246*, 369−371.

(11) Miremadi, B. K.; Morrison, S. R. *J. Appl. Phys.* **1990**, *67*, 1515−1520.

(12) Miremadi, B. K.; Cowan, T.; Morrison, S. R. *J. Appl. Phys.* **1991**, *69*, 6373−6379.

(13) Danot, M.; Mansot, J. L.; Golub, A. S.; Protzenko, G. A.; Fabritchnyi, P. B.; Novikov, Y. N.; Rouxel, J. *Mater. Res. Bull.* **1994**, *29*, 833−841.

(14) Tenne, R.; Margulis, L.; Genut, M.; Hodes, G. *Nature* **1992**, *360*, 444−446.

(15) Homyonfer, M.; Alperson, B.; Rosenberg, Y.; Sapir, L.; Cohen, S. R.; Hodes, G.; Tenne, R. *J. Am. Chem. Soc.* **1997**, *119*, 2693−2698.

(16) Tenne, R.; Margulis, L.; Hodes, G. *Adv. Mater.* **1993**, *5*, 386-388.

(17) Hershfinkel, M.; Gheber, L. A.; Volterra, V.; Hutchison, J. L.; Margulis, L.; Tenne, R. *J. Am. Chem. Soc.* **1994**, *116*, 1914−1917.

(18) Feldman, Y.; Wasserman, E.; Srolovitz, D. J.; Tenne, R. *Science* **1995**, *267*, 222−225.

(19) Feldman, Y.; Frey, G. L.; Homyonfer, M.; Lyakhovitskaya, V.; Margulis, L.; Cohen, H.; Hodes, G.; Hutchison, J. L.; Tenne, R. *J. Am. Chem. Soc.* **1996**, *118*, 5362−5367.

(20) Margulis, L.; Dluzewski, P.; Feldman, Y.; Tenne, R. *J. Microsc.* **1996**, *181*, 68−71.

(21) Homyonfer, M.; Mastai, Y.; Hershfinkel, M.; Volterra, V.; Hutchison, J. L.; Tenne, R. *J. Am. Chem. Soc.* **1996**, *118*, 7804−7808.

(22) Rapoport, I.; Bilik, Y.; Tenne, R. *Nature* **1997**, *387*, 6635−6.

(23) Sevov, S. C.; Corbett, J. D. *Science* **1993**, *262*, 880−884.

S0002-7863(97)02170-7 CCC: $15.00
Published on Web 01/13/1998

thesis. Others have examined this process as well, without realizing the ability to control the size and shape of the nanotubules or clusters.[24,25] We have demonstrated herein that by using a template, control over the size and size distribution of nanofibers or tubules of MoS_2 could be achieved through more delicate means.

The use of a template to form nanoparticles of materials is not a concept that is unique to us.[26−39] Indeed, an entire issue of *Chemistry of Materials*, Volume 8, issue 8, has been dedicated to reviewing nanocluster chemistries including the use of templates to prepare nanostructures of materials such as nanotubular graphite.[40] Our unique contribution to this chemistry has been to utilize the low-temperature reactions of Müller[41−43] to produce MoS_2 from solution-phase precursors within the porous template of electrochemically-generated aluminum oxide membranes.[44,45] It has been demonstrated that ammonium thiomolybdates will decompose to form MoS_2 and gaseous byproducts, reactions 1 and 2. Differential thermal analysis (DTA), thermogravimetric analysis (TGA), temperature programmed reduction (TPR), and X-ray diffraction have been used to monitor the decomposition processes;[41−43,46] the decompositions of both $(NH_4)_2MoS_4$ and $(NH_4)_2Mo_3S_{13}$ occur within 1 h at 450 °C in a H_2/N_2 atmosphere to form MoS_2:

$$H_2 + (NH_4)_2MoS_4 \rightarrow MoS_2 + 2NH_3 + 2H_2S \quad (1)$$

$$6H_2 + (NH_4)_2Mo_3S_{13} \rightarrow 3MoS_2 + 2NH_3 + 7H_2S \quad (2)$$

We report herein that the soluble ammonium thiomolybdate precursors of Müller have been incorporated into well-defined porous aluminum oxide membrane templates. The cylindrical pores sizes and size distributions within these membranes are controllable[44,45] with diameters ranging from 50 to 330 nm for this study and lengths approaching 30−60 μm; consequently, the size and shape of the MoS_2 tubules and fibers prepared therein are dictated and could be controlled by the template. The shapes, sizes, and morphologies of these MoS_2 nanoscale particles have been studied as a function of solvent, solution precursor, reaction conditions, and template pore sizes.

Experimental Section

Materials. $(NH_4)_2MoS_4$ was provided by the Exxon corporation, $(NH_4)_2Mo_3S_{13}$ was prepared as described by literature methods[47] and was characterized by infrared spectroscopy. All distilled water used was purified and deionized (to 18 MΩ) with a Barnstead NANOPure water purification system. Aluminum oxide templates were either purchased or prepared by standard methods.[44,45] Templates with large pore diameters were obtained from Whatman International Ltd. (aluminum oxide membranes sold as having 0.2 μm pores have measured inner pore diameters of 0.33 ± 0.04 μm) and lengths as long as 60 μm. Templates with pore diameters of 50 ± 5 nm were synthesized in the C. R. Martin laboratory at Colorado State. The general procedure for the growth of thin porous sheets of aluminum oxide was as follows: two aluminum plates, 14 cm × 5 cm × 2 mm were used as an anode in a 4% oxalic acid bath at 3−10 °C and were electrolyzed at a constant voltage of 40 V. Growth of the porous oxide was continued for 10 h to obtain a 30 μm thick sheet of amorphous aluminum oxide with pore diameters of 50 nm. The template was removed from the aluminum plate by gradually reducing the cell voltage (to ∼2−4 V) and soaking the electrode for several hours in a room-temperature solution of 25% sulfuric acid. After the oxide detached from the electrode, the colorless membranes were rinsed several times with deionized water and broken into small pieces (∼0.5 cm^2) for the templating reactions.

Reactions. Stock solutions of the $(NH_4)_2MoS_4$ thiomolybdate precursor were prepared in the solvents of choice (dimethylformamide (DMF), ethylenediamine (en), pyridine (py) (0.034 M was saturated), dimethyl sulfoxide (DMSO)), and all solutions were filtered through a fine glass frit to ensure that the solids had dissolved in the dark red-brown solutions. Stock solutions of the $(NH_4)_2Mo_3S_{13}$ precursor were generally less concentrated (0.05 M) due to saturation of the solvents. General introduction of the precursor solution was accomplished by dipping a 5 × 5 mm piece of the template into the appropriate thiomolybdate solution (alternative methods are described in the Results and Discussion section, 2.A, *vide infra*). The solvent was evaporated to dryness on a 70 °C hot plate in air. The loaded template was placed on a stage in a fused silica flow-through tube and placed in a tube furnace. An atmosphere of 10% H_2/N_2 was introduced into the tube flowing at a rate of 20 mL/min while the template was heated at 10 deg/min to 450 °C. The furnace was held at this temperature for 1 h before step cooling to room temperature. During the heating process, the reddish brown color of the precursor-laden templates turned to the expected black color of MoS_2.

Sample Characterization. UV−visible absorbance spectroscopy was performed on a Hitachi U-3501 spectrometer within the spectral range 300−800 nm. Specimens for transmission electron microscopy (TEM) and electron diffraction were prepared by dissolving away the aluminum oxide membrane. This was accomplished by placing a ∼2 mm^2 section of the template containing the products in a 1 M solution of NaOH that was left undisturbed for 30 min. The solution was slowly removed via syringe and was carefully replaced with distilled water to rinse the product. The rinse step was repeated two more times. The remaining black solid was collected on a Formvar-coated copper TEM grid and was allowed to air-dry before analysis. Images were obtained in a JEOL JEM 2000EX II TEM working at an accelerating voltage of 100 KV. Electron diffraction patterns were collected in this instrument at a camera length of 120 cm. Specimens for scanning electron microscopy (SEM) were fixed to a piece of copper tape and soaked in 1 M NaOH for 2 h to remove the aluminum oxide template. After careful rinsing with deionized water in three static rinse baths, the tape

(24) José-Yacamán, M.; López, H.; Santiago, P.; Galván, D. H.; Garzón, I. L.; Reyes, A. *Appl. Phys. Lett.* **1996**, *69*, 1065−1067.
(25) Remskar, M.; Skraba, Z.; Cléton, F.; Sanjinés, R.; Lévy, F. *Appl. Phys. Lett.* **1996**, *69*, 351−353.
(26) Martin, C. R. *Acc. Chem. Res*. **1995**, *28*, 61.
(27) Martin, C. R. *Science* **1994**, *266*, 1961−1966.
(28) Martin, C. R. *Chem. Mater.* **1996**, *8*, 1739.
(29) Lakshmi, B. B.; Dorhout, P. K.; Martin, C. R. *Chem. Mater.* **1997**, *9*, 857−862.
(30) Zelenski, C. M.; Hornyak, G. L.; Dorhout, P. K. *Nanostruct. Mater.* **1997**, *9*, 173−176.
(31) Ozin, G. A. *Supramol. Chem.* **1995**, *6*, 125.
(32) Dag, O.; Kuperman, A.; Ozin, G. A. *Adv. Mater.* **1994**, *6*, 147−150.
(33) McMurray, L.; Holmes, A. J.; Kuperman, A.; Ozin, G. A.; Özkar, S. *J. Phys. Chem.* **1991**, *95*, 9448.
(34) Macdougall, J. E.; Stucky, G. D. In *On Clusters and Clustering: from Atoms to Fractals*; Reynolds, P. J., Ed.; Elsevier: Amsterdam, The Netherlands, 1993; pp 273−285.
(35) Herron, N.; Wang, Y.; Eddy, M. M.; Stucky, G. D.; Cox, D. E.; Moller, K.; Bein, T. *J. Am. Chem. Soc.* **1989**, *111*, 530−540.
(36) Moran, K. L.; Harrison, W. T. A.; Kamber, I.; Gier, T. E.; Bu, X. H.; Herren, D.; Behrens, P.; Eckert, H.; Stucky, G. D. *Chem. Mater.* **1996**, *8*, 1930−1943.
(37) Wang, Y.; Herron, N. *J. Phys. Chem.* **1988**, *92*, 4988−4994.
(38) Wang, Y.; Herron, N. *J. Phys. Chem.* **1991**, *95*, 525−532.
(39) Wang, Y.; Herron, N. *Res. Chem. Intermed.* **1991**, *15*, 17−29.
(40) Kyotani, T.; Tsai, L.; Tomita, A. *Chem. Mater.* **1996**, *8*, 2109−2113.
(41) Prasad, T. P.; Diemann, E.; Müller, A. *J. Inorg. Nucl. Chem.* **1973**, *35*, 1895−1904.
(42) Diemann, E.; Müller, A.; Aymonino, P. J. *Z. Anorg. Allg. Chem.* **1981**, *479*, 191−198.
(43) Müller, A.; Diemann, E.; Branding, A.; Baumann, F. W.; Breysse, M.; Vrinat, M. *Appl. Catal.* **1990**, *62*, L13-L17.
(44) Diggle, J. W.; Downie, T. C.; Goulding, C. W. *Chem. Rev.* **1969**, *69*, 365−405.
(45) Brumlik, C. J.; Martin, C. R. *J. Am. Chem. Soc.* **1991**, *113*, 3174−3175.
(46) Brito, J. L.; Ilija, M.; Hernandez, P. *Thermochim. Acta* **1995**, *256*, 325−338.
(47) Hadjikyriacou, A. I.; Coucouvanis, D. *Inorg. Synth.* **1990**, *27*, 39−53.

was attached to an SEM stub and was sputtered with a 5 nm layer of gold. Images were obtained with use of a Philips 505 SEM operating at an accelerating voltage of 30 KV and a spot size of 15 nm. Energy dispersive spectroscopy (EDS) was performed in the microscope with use of a Kevex Super 8000 analyzer.

Results and Discussion

1. Fiber Characterization. In all cases, firing the precursor-laden templates at 450 °C in a 10% H_2/N_2 atmosphere for 1 h yielded dark black or brown templates. These observations were made regardless of the method by which the templates were impregnated by the various thiomolybdate solutions, see Section 2, below. Thus, either dipping the templates into ammonium thiomolybdate solutions or the dropwise application of the solutions to the templates produced darkly colored products upon heating in a reducing atmosphere. Analyses of the membranes by electron microscopies, by EDS, and by optical absorption spectroscopy revealed that the black material within the pores of the template was MoS_2. Furthermore, the morphology of the MoS_2 produced within the template was affected by the solution characteristics (concentration, solvent type) and the pore diameters of the templates. Microanalysis by energy dispersive spectroscopy in the SEM showed a single peak at 2.3 keV, the energy expected for both the sulfur K_α and the molybdenum L_α emissions. Because these elements both produce X-rays of the same energy upon excitation with an electron beam, it was not possible to use these data to calculate the stoichiometry of Mo:S in our fibers. This experiment did confirm, however, the absence of other impurities in the MoS_2.

A. Structural Characterization. Initial SEM imaging of the samples before dissolution of the templates did not reveal dramatic changes in the overall appearance of the samples following the heat treatments. In fact, there appeared to be very little material (MoS_2) that had accumulated on the surface of the templates, and the pores were still visible on the surface of the template. Even when the templates were broken to reveal the inner surfaces of the pores, the pores appeared to be hollow. However, when the aluminum oxide template was removed by dissolution treatments with 1.0 M NaOH solutions, fibers of MoS_2 that appeared as a "negative image" of the porous template were observed. The SEM image shown in Figure 1 reveals that the fibers are, in general, intact throughout the lengths of the pores even after the membrane template is removed. The fibers in this image were prepared with 0.1 M $(NH_4)_2MoS_4$ DMF solutions. The fibers in Figure 1 are 30 μm long and 50 nm wide and do not stand erect as bristles of a brush but appear more flexible, like straw.

Imaging by TEM revealed that the fibers observed in the SEM images were actually hollow tubules of MoS_2, tubules that are reminiscent of Tenne's MoS_2 nanotubules prepared by high-temperature (>800 °C) gas-phase reactions of MoO_3 and H_2S.[14] A typical TEM image of the MoS_2 fibers is shown in Figure 2. The fibers in this image were prepared with 0.1 M $(NH_4)_2MoS_4$ DMF solutions. These fibers were isolated from the template by the dissolution of the aluminum oxide by 1.0 M NaOH solutions as mentioned above. Another image of the fibers shows an end-on view and confirms the hollow nature of the fibers, Figure 2b, where there is greater electron density on the edges of the fibers than in the center. The wall thickness of the tubules was determined with use of high magnification (500000×) TEM imaging, wherein the individual layers of MoS_2 could be observed and counted, Figure 3. Tubules prepared with a 50 nm diameter porous membrane displayed wall thicknesses that ranged from ~2 to 13 ± 1 nm (4−22 layers of MoS_2).

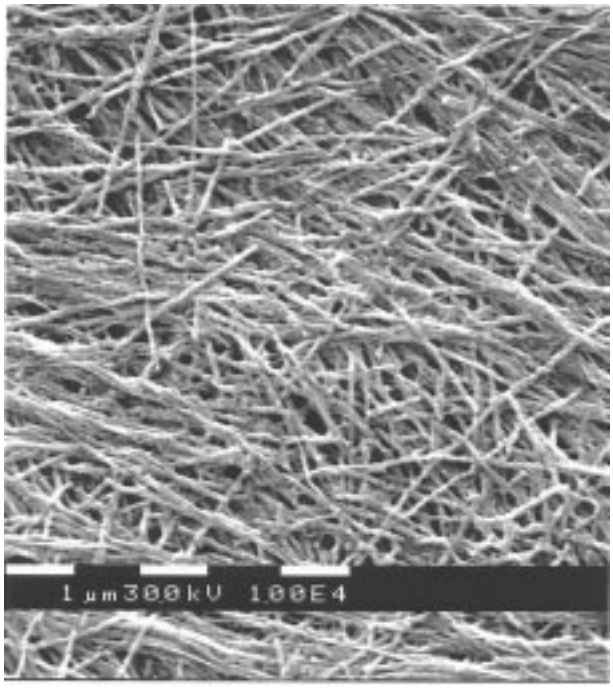

Figure 1. An SEM micrograph of the MoS_2 fibers after dissolution of the aluminum oxide template. The magnification is 10000×.

Another interesting observation about the morphology of the tubules is also illustrated in Figure 2. Regions of high electron density appear along the tubules and transect the hollow regions of the tubes at apparently regular intervals of 70−110 nm. High magnification TEM, together with stereoimagery, confirmed that these are blockages along the tubules. Figure 3 also shows that the MoS_2 layers curve along the transecting region, extending out from the surface of the tubule. These are relatively thin formations that contain 12−15 MoS_2 layers and do not appear to be merely gradual thickening of the tubule walls but are rather unique formations that are reminiscent of Tenne's hollow "nested fullerene" formations of MoS_2 and WS_2[14,16] and Kyotani's graphite tubules.[40]

Attempts were made to investigate the structure of the tubules *in situ* within the template by powder X-ray diffraction (XRD), but poor quality patterns were observed presumably because insufficient quantities of MoS_2 existed within the template. The XRD pattern from bulk precursor decomposed in 10% H_2/N_2 at 450 °C, Figure 4, is consistent with the observations made by Müller[41] and indexed to an hexagonal cell with lattice parameters $a = 3.151(4)$ Å and $c = 12.78(6)$ Å.

The structural nature of the tubules was investigated by electron diffraction. A typical electron diffraction pattern of a selected region of the tubules is shown in Figure 5, together with the fibers and their orientation (75000× magnification). All of the powder rings resulting from the electron diffraction could be indexed to the pattern of 2H−MoS_2 by using the method of comparative *d* spacings.[48,49] Careful scrutiny of the powder patterns revealed a preferential orientation of the crystallites that is manifested in the intensities of several reflections parallel and perpendicular to the tubule axis. Diffraction from the (00*l*) family of planes occurs only perpendicular to the tubule axis, suggesting that this family of planes is parallel to the tubule surface or that the MoS_2 layers are

(48) JCPDS file No. 37-1492.
(49) Edington, J. W. *Electron Diffraction in the Electron Microscope*; MacMillan Press: London, 1975.

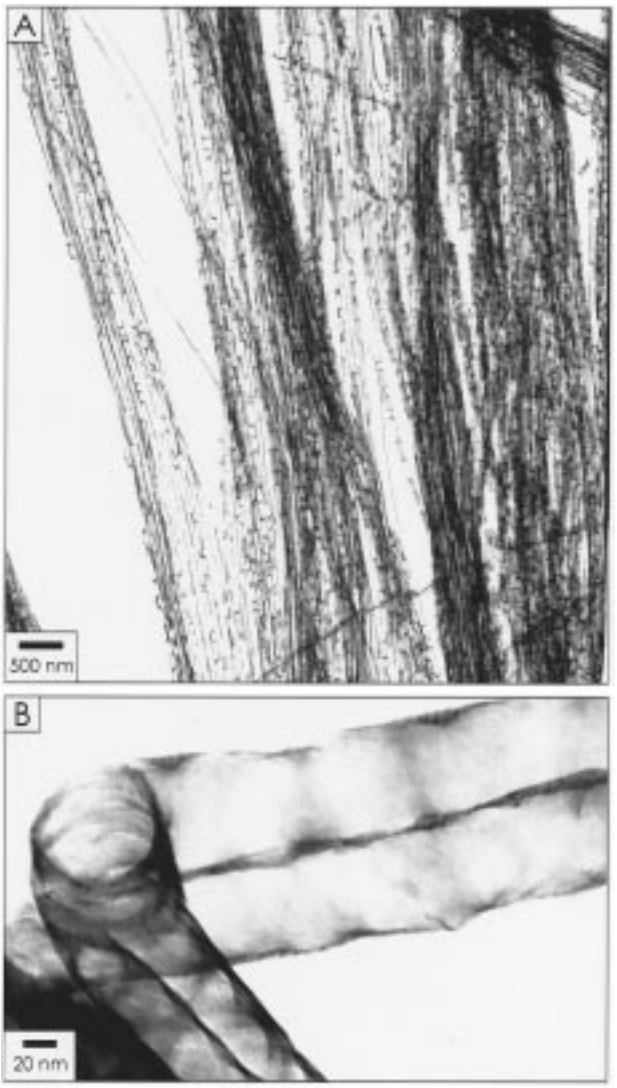

Figure 2. (A) A TEM image of the MoS_2 tubules after dissolution of the aluminum oxide template. The magnification is 12000×. (B) A TEM image of a bend in a tubule of MoS_2 emphasizing the hollow nature of the tubules. The magnification is 200000×.

stacked parallel to the tubule surface, consistent with the observation made at high magnification, Figure 3. Other electron diffraction spots, such as the (103) reflection, also showed directional variations in intensity; these were relatively easy to observe on the negative, but were more difficult to observe in the printed image, Figure 5. The preferential orientation observations are also consistent with Tenne's MoS_2-tubule formation.[18]

B. Optical Characterization. Optical characterization of the films was done by UV−visible absorption spectroscopy. An appropriate amount of MoS_2 was formed in the template to absorb significantly, between 0.5 and 1.0 absorbance units in the range from 300 to 800 nm. The template was not dissolved away from the MoS_2 fibers as it acted as a sample holder. A typical absorption spectrum is shown in Figure 6. This sample was prepared by the repeated dipping and firing process described below in Section 2.A as the "dip-dry-dry" method. Throughout the optical range studied, the aluminum oxide template did not absorb significantly except at wavelengths less than ∼350 nm where it absorbed strongly. These spectra typically displayed a strong, broad absorption with a maximum centered at 380 nm and two much weaker absorptions at 604 and 660 nm.

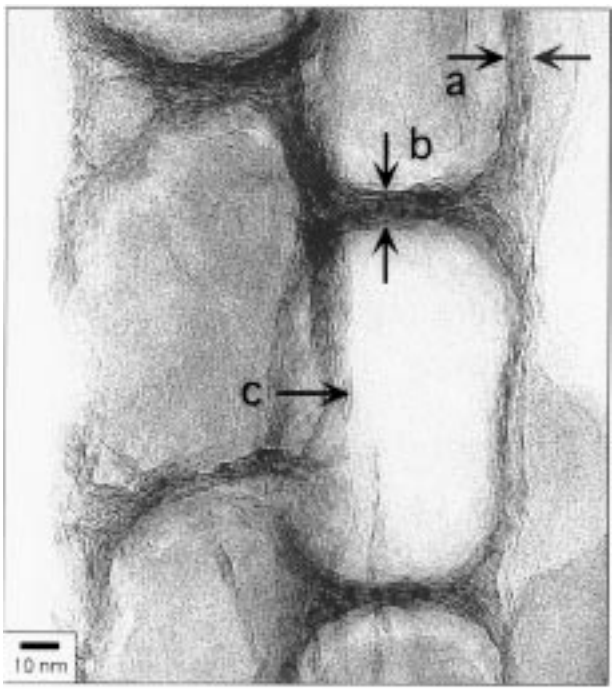

Figure 3. A high magnification image (500000×) of the tubules of MoS_2. The two arrows labeled (a) show the tubule wall thickness and the two arrows labeled (b) show the transecting region of the tubule. Arrow (c) points to an individual MoS_2 layer.

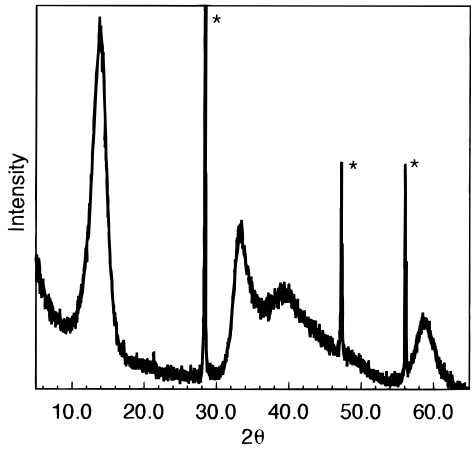

Figure 4. The XRD pattern for the product resulting from the thermal decomposition of bulk $(NH_4)_2MoS_4$ in 10% H_2/N_2 at 450 °C. Peaks labeled with an asterisk are driffraction peaks from an internal Si standard.

The general appearance of our spectral data is similar to that of bulk MoS_2, which possesses an intense absorption in the blue region of the spectrum and weaker absorbances in the red region. Single-crystal absorption data reported by Evans and Young[50] showed strong, broad absorption peaks centered at 397 and 448 nm; the data for our tubules show only one broad peak near 380 nm. Evans and Young also reported two smaller but sharper peaks at lower energy at 598 and 658 nm in room-temperature spectra. Our tubules display two weaker peaks in this area. Although these peaks are weak and somewhat broad, their positions were reproducible and compare well with those of the bulk spectrum.

Our data do appear to be shifted with respect to the data obtained by Tenne from their MoS_2 nanoparticles.[19,51] In their

(50) Evans, B. L.; Young, P. A. *Proc. R. Soc. London, Ser. A* **1965**, *284*, 402−422.

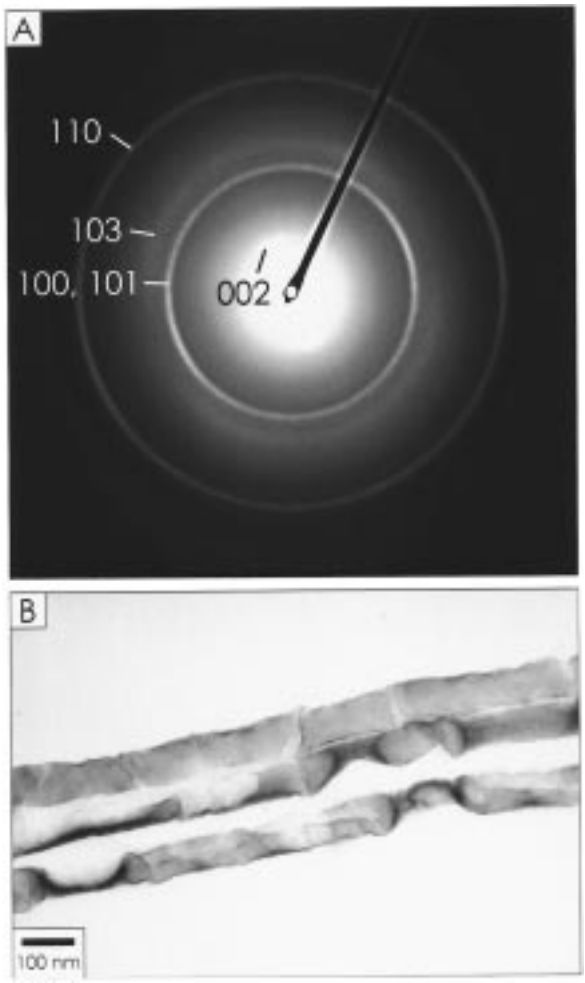

Figure 5. (A) An electron diffraction pattern from the tubules in (B). The orientation of the diffraction image and the tubules are identical. Miller indices of the indexed lines are given.

reports, they described two peaks in the low-energy region of the spectrum, at 616.3 and 667 nm, as well as a third, very broad and noisy peak at 525 nm. It should be noted that the data obtained by Tenne were obtained at low temperatures, while our data were collected at room temperature.

Although the bulk single-crystal optical absorption spectrum of MoS_2 has been carefully studied and the peaks assigned to specific transitions, the spectral behavior of nanocrystalline MoS_2 has not been thoroughly explained as a function of the particles' size and shape,[52] although recent studies have been made by Wilcoxon et al.[53] and Tenne et al.[51] Wilcoxon examined the electronic band structure of nanoparticles (2−5 nm) of MoS_2 and made some assignments based on Wold's previous spectroscopic analysis.[54] Tenne has studied the low energy exciton peaks and presented electronic band structures based on two adjacent MoS_2 slabs which help to confirm the nature of the two low energy peaks.[51] The spectral signature of our tubules falls within a region bounded by bulk and nanocluster; moreover, we cannot discount the possibility that the shifts from nanocluster spectra may be due to the formation of H_xMoS_2 instead of MoS_2, *vide infra*, Section 2.G.

2. Variations in Reaction Conditions. The conditions of loading and decomposing the molybdate precursors within the

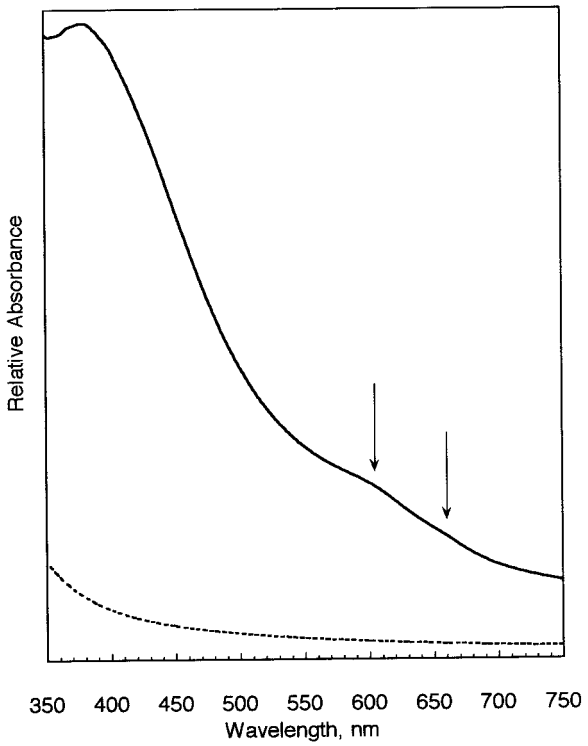

Figure 6. The optical absorption spectrum of a typical 50 nm tubule sample. The two arrows denote the weak absorptions in the red region of the spectrum described within the text. The dashed-line spectrum shows the absoprtion of the template on the same scale.

porous template were varied in an attempt to understand how the fibrous tubules of MoS_2 grew and whether there could be any control of the morphology of the fibers produced. Variations in the conditions included altering the method of precursor incorporation into the pores of the templates, the molybdate source (using $(NH_4)_2Mo_3S_{13}$ versus the $(NH_4)_2MoS_4$ precursor), the solvent system, the precursor concentrations, the template pore size, and the firing conditions.

A. Incorporation Methods. The precursor of choice was introduced, initially, by repeatedly dipping the template into a precursor solution and allowing the solvent to dry between dipping (see Experimental Section, *vide supra*). After a prescribed number of "dip-and-dry" cycles, the precursor-laden templates were fired, as described earlier. A second method using highly concentrated solutions was investigated. This method involved placing the template on a 70 °C hot plate and slowly dripping the precursor solution onto it. After each drop was added, the solvent was allowed to evaporate, leaving behind the thiomolybdate in the pores of the template ("drip-and-dry"). SEM analysis of the template after firing revealed that a layer of MoS_2 built up on the outer surface and blocked the entrance to the pores. To complicate matters, it appeared that the pores had not been filled completely, top to bottom, by the solution before the top surface of the template became coated by precursor; nevertheless, hollow tubules formed with characteristics similar to those reported for the "dip-and-dry" method.

A third method for incorporating the precursor into the pores was tested that attempted to fill the pores before the ends were plugged by the template surface layer as observed in the dropwise addition method described above. In this method, the template was dipped in the precursor solution and the excess

(51) Frey, G. L.; Elani, S.; Homyonfer, M.; Feldman, Y.; Tenne, R. *Phys. Rev. B* In press.
(52) Parsapour, F.; Kelley, D. F.; Craft, S.; Wilcoxon, J. P. *J. Chem. Phys.* **1996**, *104*, 4978−4987.
(53) Wilcoxon, J. P.; Newcomer, P. P.; Samara, G. A. *J. Appl. Phys.* **1997**, *81*, 7934−7944.
(54) Coehoorn, R.; Haas, C.; Dijkstra, J.; Flipse, C. J. F.; deGroot, R. A.; Wold, A. *Phys. Rev. B* **1987**, *35*, 6195−6203.

solution on the membrane surfaces was absorbed with a Kimwipe. After this surface solution was removed, the membranes were dried at 70 °C. This method was known as the "dip-dry-dry" method. Repeated dipping and drying was performed before firing the templates. We observed that the tubules produced by this method were not significantly different from those described for the "dip-and-dry" or the "drip-and-dry" methods above.

A fourth method for incorporating the precursor into the pores was tested to determine if thicker-walled tubules or solid fibers of MoS_2 could be produced. The entire process of dipping the template once into the precursor solution, drying, and firing the membrane was repeated 15 times with one sample, becoming known as the "dip-fire-dip" process. As in the "dip-and-dry" method, this process formed tubules of MoS_2 that were plugged at points along the tubule. In addition, MoS_2 formed on the outer surface of the template, indicating that the tubules may become plugged during the first firing and that additional dipping attempts did not load a significantly greater quantity of the precursor into the pore but rather primarily covered only the outer surface of the template; however, repeated firings did result in visibly "stiffer" tubules as evidenced by the erect nature of the tubules imaged in the TEM.

B. Precursor Selection. The reactions of either molybdenum precursor yielded essentially morphologically identical results. According to Müller, both of these precursors are known to decompose under reducing conditions at elevated temperatures.[41−43,55] Tubules that resulted from reactions using the $(NH_4)_2Mo_3S_{13}$ cluster as a molybdenum source were almost identical with those formed from the $(NH_4)_2MoS_4$ precursor. The difference noted was that the tubules formed from the $(NH_4)_2Mo_3S_{13}$ cluster precursor showed longer hollow regions along the fiber axis. Plugs transecting the tubes, *vide supra*, were found with both precursors.

C. Solvent Effects. Several other polar solvent systems besides DMF were considered for solvent dependence studies: (py), DMSO, and (en). The template studied contained 50 nm pores, and the method of loading the template was the "dip-and-dry" method described above with 0.1 M thiomolybdate solutions. One exception to that was the pyridine solutions, which saturated at 0.034 M. Figure 7 compares TEM images of the MoS_2 fibers produced by using each of the solvents in question. Similar morphologies were found for most of the fibers produced with (py), DMSO, and DMF solutions. The fibers produced with (en) solutions were more dense than the others and broke into short pieces (∼150−700 nm in length). All of these observed morphologies are similar to the morphologies of carbon nanotubules prepared by firing poly(furfuryl alcohol) in aluminum oxide templates at 2800 °C.[40] In this report by Kyotani et al., they did not offer an explanation for their observations.

We believe that the morphologies of the MoS_2 fibers resulting from our processes were indicative of the shape of the thiomolybdate precursor remaining within the confining template after the solvent had evaporated. In the studies that have reported the decomposition of these precursors,[43,55] no evidence was reported for the large-scale rearrangement or annealing of the MoS_2 solid during the reaction at 450 °C. Müller did observe in both scanning tunneling microscopic (STM) and high-resolution TEM studies of their decompositions that very small particles of MoS_2 could be found. In general, they observed that particles with average sizes of 5.5 nm formed on alumina catalyst supports by a method similar to our "drip-and-dry" method (no. 2). Müller did not report observing any structures remotely similar to our tubules. Their STM studies followed the decomposition reactions on a surface in situ, wherein they observed that a thick layer (100 nm) of deposited precursor (thiomolybdate/DMF on highly oriented pyrolytic graphite) decomposed into particles of MoS_2 of the dimensions $100 \times 100 \times 50$ nm. They suggested that although there was some crystalline product formation, the molybdate precursor did not migrate far along the surface to form the crystallites. In our studies, we would expect, based on Müller's observations, that the formations we observed within the tubules of the MoS_2 resulted from the evaporation dynamics of the solvent−precursor mixture rather than any annealing process of the MoS_2 that had been formed. Thus, the unique shapes of MoS_2 produced by our reactions likely reflect the shape of the thiomolybdate precursor left behind in the template after the solvent evaporated.

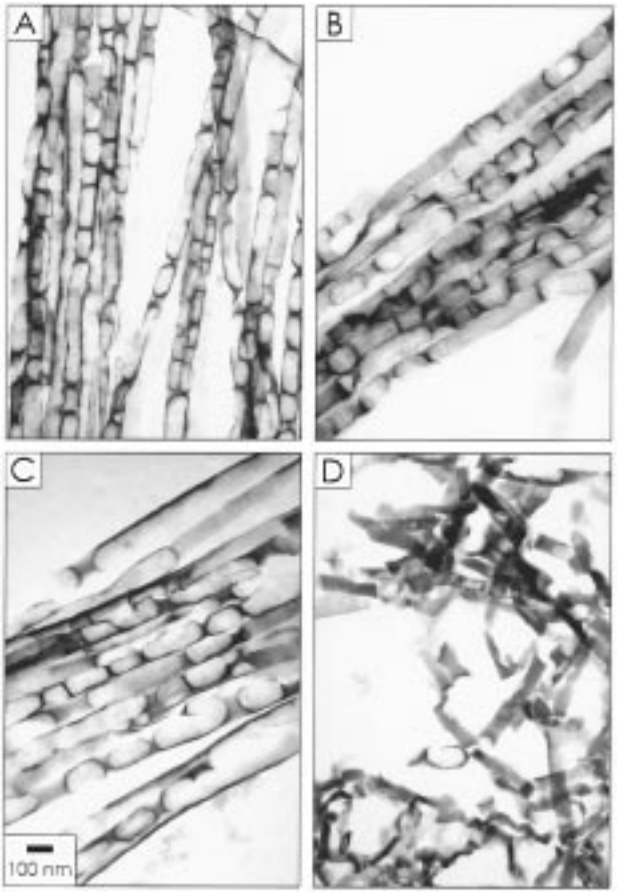

Figure 7. TEM images A through D illustrate the effects of precursor solution solvent on the morphology of the tubules of MoS_2 prepared from 50 nm templates: fibers from DMF solutions (A), DMSO solutions (B), py solutions (C), and en solutions (D). The images were all taken at the same magnification, 50000×.

The evaporation of a solvent on a surface is itself a complex process, and several recent studies have reported on the evaporation of pure solvents from a wettable surface.[56−59] These reports indicated that as the solvent evaporated, the liquid remaining formed complex two-dimensional patterns. The forces that generated these patterns are not yet completely

(55) Diemann, E.; Branding, A.; Müller, A. *Bull. Soc. Chim. Belg.* **1991**, *100*, 961−966.

(56) Redon, C.; Bouchard-Wyart, F.; Rondelez, F. *Phys. Rev. Lett.* **1991**, *66*, 715−718.

(57) Fournier, J. B.; Cazabat, A. M. *Europhys. Lett.* **1992**, *20*, 517−522.

(58) Elbaum, M.; Lipson, S. G. *Phys. Rev. Lett.* **1994**, *72*, 3562−3565.

(59) Elbaum, M.; Lipson, S. G. *Isr. J. Chem.* **1995**, *35*, 27−32.

understood. Comparing these studies to the behavior in our thiomolybdate reactions presented several concerns. Our thiomolybdate systems included two elements of added complexity: the evaporation or drying of saturated thiomolybdate solutions was more complex than that of pure solvents (i.e. ours were binary systems), and the small pores of the templates allowed or promoted the formation of three-dimensional patterns as the solvent evaporated versus the evaporation from flat surfaces. It is likely that the imperfections in the surface of the template (the error in observed pore diameter is approximately 10%) play a role in the effects of wetting by creating a meniscus at points along the pore which, when fired, creates the transecting regions of the tubules. We cannot, however, offer a definitive explanation for the many different formations seen resulting from different solvent systems. These observations are, however, the focus of our continuing examinations of this method for preparing uniform, homogeneous fibrous and tubular MQ_2 solids such as WS_2, ReS_2, and TiS_2 by precursor decomposition methods.[60]

D. Concentration Effects. A solution (0.01 M) of $(NH_4)_2MoS_4$ in DMF was used for the dipping process described earlier to determine the effects of concentration on the formation of MoS_2 tubules. The template was dipped 15 times in the thiomolybdate solution, using the "dip-and-dry" method followed by firing. The fibers that formed were not significantly different from those described above. Tubules with wall thicknesses similar to those produced from solutions of 0.1 M thiomolybdate were observed; these also displayed multiple plugs inside each tubule. Thus, even when a low concentration of the precursor was used to form fibers, the formation of plugs inside the tubules could not be avoided.

When the template was dipped only one time in a 0.01 M thiomolybdate solution, only a small amount of thiomolybdate was loaded into the template. In these cases, tubules did not form, but rather narrow sheets of MoS_2 formed that extended along one wall of the pores. These sheets, as observed by TEM, were roughly the same width as the template's pores, but they were not tubular. These observations suggest that the MoS_2 is more likely to grow along the length of the pore than around its circumference when there is not enough material present to form the entire tubule.

E. Pore Size Effects. Changing the template pore size from 50 to 330 nm diameters significantly changed the morphology of the resulting fibers. Long fibers (10−30 μm) similar to those produced in the narrow templates were produced, as seen in SEM, but TEM imaging showed that these fibers displayed different morphologies than those made in the narrower templates. Fibers made in the larger pore templates displayed some small sections, ∼1 μm long, that appeared as hollow tubules, but the majority of fibers had formed as partial tubules or as a thick section or film of MoS_2 along one side of the pores, as seen in Figure 8. These thicker sections of MoS_2 were generally ∼170−230 nm wide. Stereoimages obtained in the TEM confirmed that these sections were not round fibers, but films that had formed along one side of the pore. These films appeared curved and split lengthwise along the length of the fiber. The surface of the MoS_2 films was jagged and uneven, resembling the surface of MoS_2 observed in Müller's thermal decomposition of a thin film of thiomolybdate precursor on a flat surface.[55] Dimples were also observed in the surface of these fibers. All of these observations suggest that as the template pores become large enough, above 300 nm, intact tubules of MoS_2 can no longer be formed and the control of tubule size and morphology is lost—the precursors simply decompose into films of MoS_2 rather than tubules.

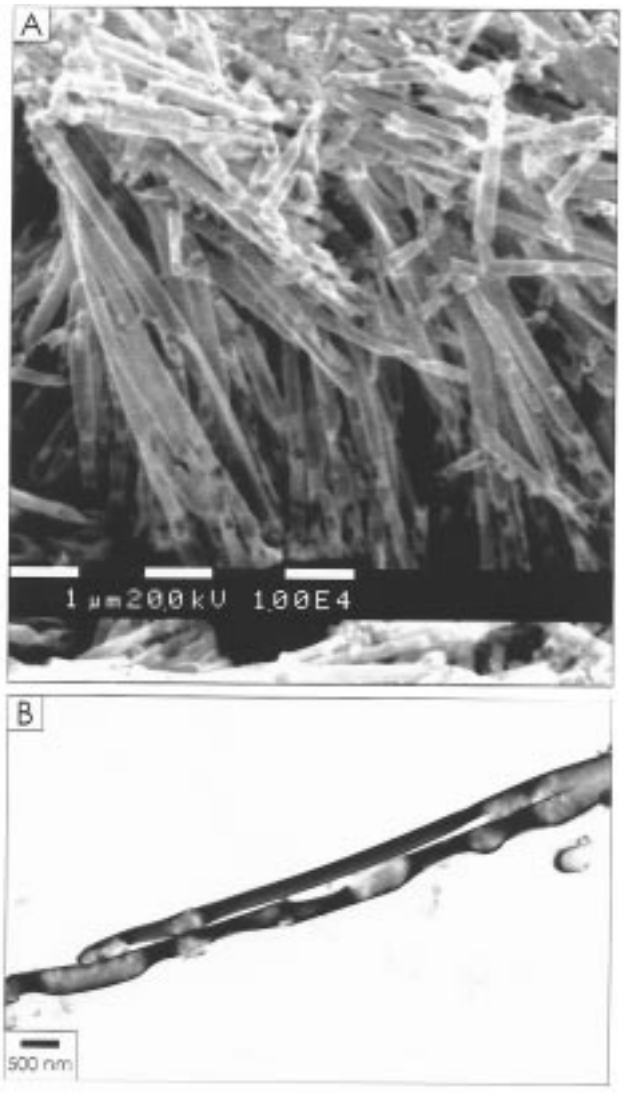

Figure 8. (A) An SEM image of the fibers grown in large pore (330 nm) aluminum oxide after the template was dissolved away. (B) A TEM image of two isolated fibers showing regions that are solid (filled) and hollow (incompletely filled).

F. Heat Treatment—Annealing. In their studies of MS_2 nanoclusters, Tenne observed that annealing fullerene-like clusters at temperatures above 850 °C yielded changes in the crystallinity of the products obtained.[17,19] Tubules of MoS_2 were isolated from our template by dissolution in basic solutions by a manner similar to that used to prepare TEM samples described in the Experimental Section. It was necessary to remove the tubules from the template as firing the template caused the formation of crystalline Al_2O_3 which destroyed the structural integrity of the MoS_2 tubules. The tubules were collected on a silica microscope slide and dried before firing. Samples of MoS_2 tubules were fired at 900 °C for 90 min under a nitrogen atmosphere. The tubules were collected on a TEM grid and examined at high magnification. The TEM image reproduced in Figure 9A shows a section of one tubule. The tubule appears more crystalline than the image in Figure 3; more order can be seen in the MoS_2 layers and the tubule appears faceted much like Tenne's nested fullerene-like clusters. An electron diffraction pattern of this tubule is seen in Figure 9B. The pattern could again be indexed to 2H−MoS_2 and shows a much higher

(60) Zelenski, C. M.; Dorhout, P. K. Manuscript in preparation.

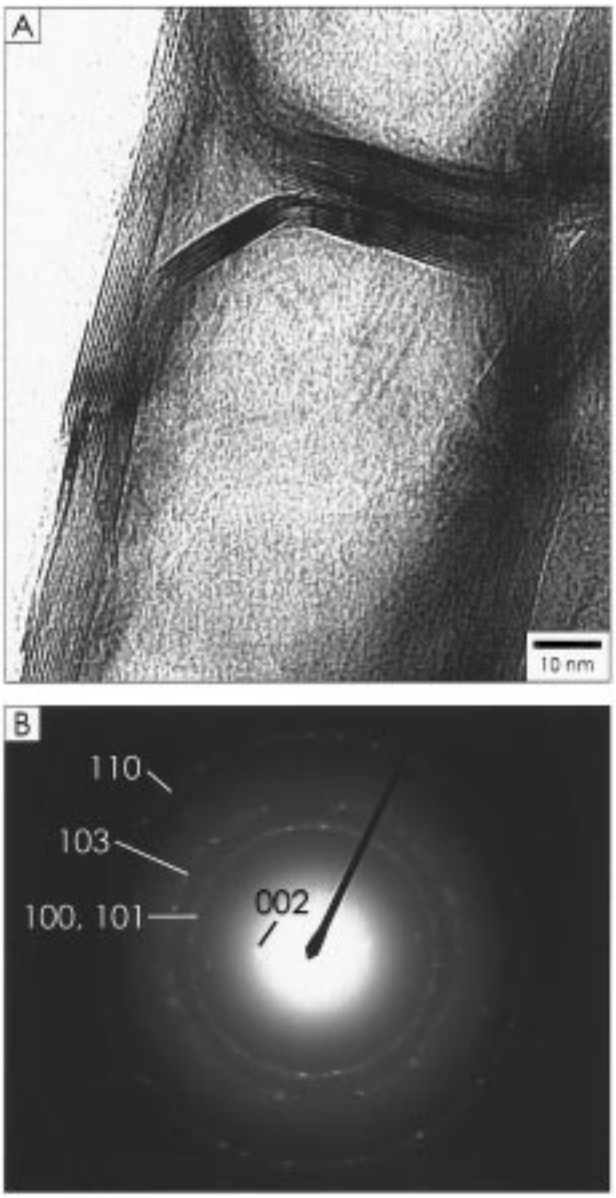

Figure 9. (A) A TEM image of the tubules annealed at 900 °C. (B) An electron diffraction pattern from the tubule in part A showing the indexed powder diffraction rings.

crystallinity as suggested by the diffraction spots along the powder rings. For the sake of comparison, XRD patterns of the bulk, heat-treated $(NH_4)_2MoS_4$, heated at annealing temperatures in an N_2 atmosphere, displayed sharper powder patterns than those from powder fired at 450 °C, which could be refined to an hexagonal cell where $a = 3.165(3)$ Å and $c = 12.584(3)$ Å.

G. Other Considerations. Hydrogen adsorption onto metal sulfides is known in the catalysis of the decomposition of heterocyclic hydrocarbon compounds.[61] The active hydrogen−MoS_2 species for this process has been debated, but several recent studies have shed light on the identity of those species.[62−66] Structural studies have revealed that a significant portion of the H_xMoS_2 solids are hydrogen intercalated MoS_2.[66] Neutron diffraction studies of H_xMoS_2, $x = 0.067$, found an interlayer d_{002} spacing of 6.389(6) Å, which is slightly larger than the accepted 6.15 Å for MoS_2. The conditions under which these solids were prepared are similar to those reported in this paper for the formation of our tubular MoS_2. Consequently, the true chemical identity of the MoS_2 tubules is in question.

In the case of our bulk $(NH_4)_2MoS_4$ heated at 450 °C in a 10% H_2/N_2 gas stream, our XRD data revealed an interlayer d_{002} spacing of 6.392(7) Å. Heating bulk $(NH_4)_2MoS_4$ under N_2 at 800 °C yielded a solid with a d_{002} spacing of 6.292(3) Å. The known H_xMoS_2 samples examined by diffraction were prepared by the action of H_2 on MoS_3 at 400 °C for 19 h.[66] In later work by Wright et al., H_xMoS_2 was prepared by the action of 20% H_2/H_2S at 250 °C on MoS_2; the resulting XRD pattern displayed a new d_{002} spacing line that appeared at 7.8 Å.[65] Still other phases of H_xMoS_2 have been reported, prepared in molten alkali halides where the *c*-axis refined to 17.97 Å.[67]

On the basis of these studies and others, we can conclude that MoS_2 will likely sorb hydrogen under a variety of conditions, including those under which we prepared our MoS_2 tubules. Our XRD data are consistent with the formation of some H_xMoS_2 in the bulk reactions studied, but we have not attempted to determine the amount of hydrogen that may have been incorporated into the solid. Neither Müller nor Tenne have addressed the possible formation of H_xMoS_2 in their work, but Tenne did observe large interlayer spacings in the XRD patterns of the fullerene-like clusters of MS_2 which he attributed to the effects of curvature on the interlayer spacing.[18] We cannot, therefore, definitively rule out the formation of H_xMoS_2 tubules versus MoS_2 tubules, but the increases in interlayer spacing may also be related to the curvature in the tubules. Moreover, the adventitious sorption of H_2 by tubules of MoS_2 to yield H_xMoS_2 could be advantageous in the application of these nanoscopic materials toward hydrodesulfurization catalysis.

Conclusions

Fibers and tubules of MoS_2 with diameters of 50 or 330 nm and lengths of 30 μm have been synthesized by loading a porous aluminum oxide template with an ammonium thiomolybdate precursor followed by controlled thermal decomposition. The MoS_2 solids evenly coated the entire inner surface of the small-pore template, yielding hollow tubules of MoS_2 of very specific diameters and wall thicknesses which appeared to be independent of the precursor choice. When larger pore templates were used, the precursors decomposed into fibers with varying thicknesses and morphologies, and a dramatic loss of controlled tubule formation was noted. The morphologies of the fibers did not depend on the concentration of the precursor solution but did depend on the type of solvent used to deposit the precursor (DMF, pyridine, ethylenediamine, or DMSO). Since the tubules appear to coat the inner surfaces of the hollow template, we would assume they must have a significantly high surface area as the templates are known to have very high surface areas.[68,69] Therefore, fibers produced by our method may be considered for use as hydrodesulfurization catalysts or as battery cathodes where a very high surface area is desirable.

(61) Badger, E. H. M.; Griffith, R. H.; Newling, W. B. S. *Proc. R. Soc. London* **1949**, *A197*, 184−193.
(62) Anderson, A. B.; Al-Saigh, Z. Y.; Hall, W. K. *J. Phys. Chem.* **1988**, *92*, 803−809.
(63) Komatsu, T.; Hall, W. K. *J. Phys. Chem.* **1991**, *95*, 9966−9974.
(64) Komatsu, T.; Hall, W. K. *J. Phys. Chem.* **1992**, *96*, 8131−8137.
(65) Sampson, C.; Thomas, J. M.; Vasudevan, S.; Wright, C. J. *Bull. Soc. Chim. Belg.* **1981**, *90*, 1215−1224.
(66) Wright, C. J.; Sampson, C.; Fraser, D.; Moynes, R. B.; Wells, P. B.; Riekel, C. *J. Chem. Soc., Faraday Trans.* **1980**, *76*, 1585−1598.
(67) Schöllhorn, M.; Kümpers, M.; Plorin, D. *J. Less-Common Met.* **1978**, *58*, 55−60.
(68) Foss, C. A.; Hornyak, G. L.; Stockert, J. A.; Martin, C. R. *J. Phys. Chem.* **1992**, *96*, 7497.
(69) Foss, C. A.; Hornyak, G. L.; Stockert, J. A.; Martin, C. R. *Adv. Mater.* **1993**, *5*, 135−136.

Further work is in progress to study the deposition and decomposition of other sulfide precursors such as thiorhenates and thiotungstates by the methods described herein and by electochemical oxidation of MS_4^{2-} in solution.[60]

Acknowledgment. Financial support for this project was provided by Colorado State University and the CSU Electron Microscopy Center, the Research Corporation Cottrell Scholar program, the Exxon Corporation (Exxon Faculty Fellowship in Solid State Chemistry), and NSF-CHE-9625378. We thank Dr. H. H. Murray, Exxon, for samples of $(NH_4)_2MoS_4$ and Prof. C. R. Martin, CSU, for use of the electrolysis equipment.

JA972170Q